Powering DNA strand-displacement reactions with a continuous flow reactor

Xinyu Cui, Dominic Scalise & Rebecca Schulman

Natural Computing
An International Journal

ISSN 1567-7818

Nat Comput
DOI 10.1007/s11047-020-09795-2

Springer

Natural Computing
https://doi.org/10.1007/s11047-020-09795-2

Powering DNA strand-displacement reactions with a continuous flow reactor

Xinyu Cui[1] · Dominic Scalise[1] · Rebecca Schulman[1,2]

Abstract
Living systems require a sustained supply of energy and nutrients to survive. These nutrients are ingested, transformed into low-energy waste products, and excreted. In contrast, synthetic DNA strand-displacement reactions typically run within closed systems provided with a finite initial supply of reactants. Once the reactants are consumed, all net reactions halt and the system ceases to function. Here we run DNA strand-displacement reactions in a continuous flow reactor, infusing fresh reactants and withdrawing waste, enabling the system to dynamically update its outputs in response to changing inputs. Running DNA strand-displacement reactions inside of continuous flow reactors allows the system to be re-used for multiple rounds of computation, which could enable the execution of more elaborate information processing tasks, including single-rail negation and sequential logic circuits.

Keywords DNA strand-displacement · Microreactor · Microfluidics · DNA computation

DNA strand displacement (DSD) reactions are a useful mechanism for processing molecular information. They have previously been used to implement Boolean logic gates (Seelig et al. 2006a; Takahashi et al. 2005; Zhang et al. 2010; Qian and Winfree 2011; Genot et al. 2011), signal amplifiers (Seelig et al. 2006b; Zhang and Seelig 2011; Zhang et al. 2007; Chen et al. 2013a), neural networks (Qian et al. 2011), and other circuits (Chen et al. 2015; Soloveichik et al. 2010; Chen et al. 2013b; Fern et al. 2016; Srinivas et al. 2017), as well as for sensing (He et al. 2010) and directed self assembly (Zhang et al. 2013; Rogers and Manoharan 2015). However, these reactions are typically run inside of a closed reactor, without additional reactants provided after initialization. When a reaction consumes its initial reactant stock and reaches equilibrium, it ceases processing information and can no longer update its output in response to changing input conditions. Providing DSD reactions with a sustained source of reactants could enable them to operate for longer times, extending the lifespans of sensors, increasing the classes of dynamic circuits that can be implemented, and enabling the directed self-assembly of more elaborate structures.

Flow and diffusion reactors have previously been used to supply reactants to several other types of chemical reactions, including protein synthesis in artificial cells on biochips (Karzbrun et al. 2014), sustained oscillations in microfluidic flow reactors (Niederholtmeyer et al. 2013; Semenov et al. 2015, van Roekel et al. 2015), and enzymatic reactions in cascading flow cells (Moseley et al. 2014; Fratto and Katz 2015, 2016; Katz and Fratto 2017). In general, these systems operate by allowing material exchange between the reaction chamber(s) and an external flow of reactants. This continuous flow of reactants allows the system to continue to react with inputs as long as the flow is maintained, analogous to the exchange of matter between living cells and their external environments.

In this study, we ran DNA strand displacement (DSD) reactions inside a continuous-flow stirred-tank reactor that

Electronic supplementary material The online version of this article (https://doi.org/10.1007/s11047-020-09795-2) contains supplementary material, which is available to authorized users.

✉ Rebecca Schulman
rschulm3@jhu.edu

[1] Chemical and Biomolecular Engineering, Johns Hopkins University, Baltimore, MD 21218, USA

[2] Computer Science, Johns Hopkins University, Baltimore, MD 21218, USA

Published online: 03 June 2020

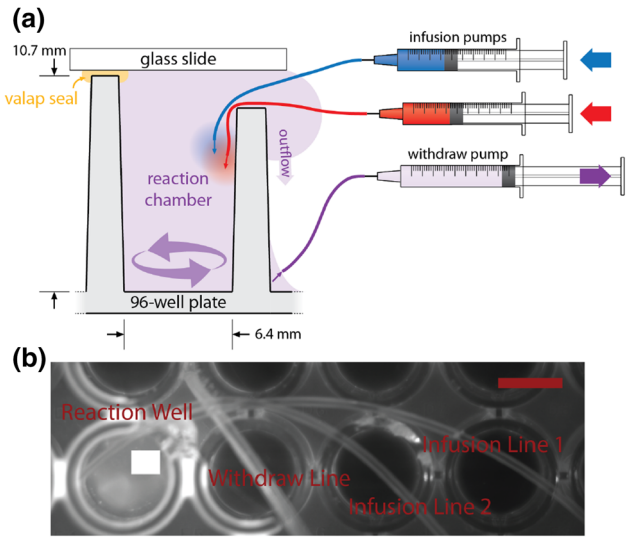

Fig. 1 Continuous-flow, stirred-tank reactor design. **a** Diagram of the side view of the reactor chamber. Infusion pumps flow reactants into one well in a 96-well plate. The solution in the well is mixed by a magnetic stir bar. A hole in the side of the chamber allows waste solution to exit the chamber, maintaining a constant reaction volume. Waste is collected from the adjacent well by a withdrawal pump. **b** Top view of the reaction chamber experimental setup. The white box indicates the imaging area. The red scale bar indicates a length of 5 mm. (Color figure online)

pumps in reactants while removing waste products (Fig. 1). We developed a simple stirred-tank flow reactor design and monitoring protocol that can be implemented without access to specialized equipment or micro-fabrication facilities. This setup can maintain reactions far from equilibrium for as long as the pumps are flowing the appropriate reactants into the reaction chamber, allowing chemical circuits to respond dynamically to changing inputs. In principle, any DSD circuit can run dynamically inside of a flow reactor. While the current iteration of the reactor does not allow molecules to be anchored within the device, it should be possible to design chemical circuits that would maintain information within the reactor permanently (SI1). In this study, we specifically demonstrate how an existing one-time-use DSD Boolean logic gate (Seelig et al. 2006a) can dynamically respond to changing input concentrations, without modification, within our reactor.

1 Reactor construction

To construct the reactor used in this study (Fig. 1), we began with a flat bottom 96-well plate. One well inside the plate was designated as the reaction chamber. A hole of about 2–3 mm in diameter was cut into the top of one side of the reaction chamber to allow fluid to flow in and out of the chamber. A stir bar (5 mm, VWR) was placed in the reactor to ensure the solution is well-mixed during the reaction. Tubing (ID 0.28 mm, Warner Instruments) attached to 25 mL syringes controlled by syringe pumps (New Era NE-300) was placed through the hole to flow reactants into the chamber. The top of the well is sealed with valap (equal parts Vaseline, lanolin and paraffin wax) and a glass slide to prevent evaporation or outflow over the top of the well. The reactor was designed so that excess liquid flowed out of the cut hole into the adjacent well, where it was collected with a withdraw pump operating at approximately 2× the volumetric inflow rate to prevent fluid buildup. The volume of the reaction chamber was measured at 380 µL. For reactions involving multiple reactants, we supplied reactants that could react with one another using different infusion lines to prevent reactions from occurring before the species reached the reaction chamber. The reactor was placed on top of a magnetic stir plate to actuate the stir bar, and fluorescence was monitored through the top of the glass slide using a gel imager. We estimate it takes approximately 30 min to fabricate each reactor chamber, at a cost of about $10 per chamber (not including the external pumps, stir plate, or gel imager).

2 Model

The rate of change of the concentration of a molecule X being pumped into the reaction chamber is:

$$\frac{d[X]}{dt} = \frac{\dot{V}_{\text{in}}}{V}[X]_{\text{in}} - \frac{\dot{V}_{\text{out}}}{V}[X] + R \tag{1}$$

where $\dot{V}_{\text{in}}$= volumetric flow rate in (units: volume/time), $\dot{V}_{\text{out}}$= volumetric flow rate out (units: volume/time), V = volume of the reaction chamber, $[X]_{\text{in}}$ = concentration of X being pumped in, R = net rate X is generated by chemical reactions in the reactor.

When the chamber is full, the escape hole cut in the side of the reaction chamber allows the same volume to escape as is pumped in. Thus in this case the volumetric flow rates are constrained to be equal (*i.e.* $\dot{V}_{\text{out}} = \dot{V}_{\text{in}}$). Substituting, we can obtain:

$$\frac{d[X]}{dt} = f_{\text{in}} - f_{\text{out}}[X] + R \tag{2}$$

where

$$f_{\text{in}} = \textit{concentration flux in} \equiv \frac{\dot{V}_{\text{in}}}{V}[X]_{\text{in}} \tag{3}$$

$$f_{\text{out}} = \textit{flux constant out} \equiv \frac{\dot{V}_{\text{out}}}{V} = \frac{\dot{V}_{\text{in}}}{V} \tag{4}$$

Solving Eq. 2 in the absence of any chemical reactions gives that when f_{in} and f_{out} are held constant, $[X]$ approaches a constant value equal to the ratio of the flux in, to the flux constant out. *i.e.*:

$$[X](t) = \frac{f_{in}}{f_{out}} + \left([X]_0 - \frac{f_{in}}{f_{out}}\right) \cdot e^{(-f_{out} \cdot t)} \quad (5)$$

$$\lim_{t\to\infty}[X](t) = \frac{f_{in}}{f_{out}} \quad (6)$$

The time that it takes for the "$[X]$" to relax from an initial concentration $[X]_0$ to a given percentage τ of the offset from steady state concentration is then:

$$t_{rise,\tau} = \frac{-\ln(\tau)}{f_{out}} \quad (7)$$

3 Control of reactant concentrations using flow alone

To test that the flow reactor operates as designed, we used a single-infusion syringe to flow in solution containing a strand of DNA, which we terned *X*, labeled with a Cy3 fluorophore (Sequence in SI Table 1) in Tris–acetate-EDTA buffer containing 12.5 mM magnesium acetate (TAE/Mg2 +), and tracked the resulting fluorescence intensity of the solution over time (Fig. 2a). The infusion line here, and in all subsequent experiments in this paper, also contained 1 μM of an inert, single-stranded DNA, consisting of twenty thiamine nucleotides to prevent the gate and input DNA from sticking to the tubes or the reactor walls (Chen et al. 2015). We tested three different volumetric flow rates ($\dot{V}_{in}$ = 10 μL/min, 20 μL/min and 40 μL/min) with two different infused concentrations of *X* ($[X]_{in}$ = 50 nM and 100 nM). We observed the fluorescence (which is assumed to be proportional to $[X]$) approaching a stable steady state controlled by the ratio $\frac{f_{in}}{f_{out}}$, with rise times controlled by f_{out}, as predicted by the model. However, when we infused a 50 nM solution of a *X* at a rate of 10 μL/min, we observed a short delay in the increase in fluorescence, which could be due to nonspecific adsorption of DNA to the pump tubing or reaction chamber. The complete materials and experimental methods are given in SI2, with our data processing procedure given in SI3.

We next asked how the concentration of *X* in the reactor changed over time and how these changes compared with the changes predicted by the model in Eq. 2 as $[X]_{in}$ is repeatedly switched between high and low concentrations. We first pumped in plain buffer from t = 0 to 1 h. We then allowed $[X]$ to equilibrate in the reaction chamber by pumping in a solution containing $[X]_{in}$ = 50 nM at 6 μL/min from t = 1 to 6 h. We then infused a buffer containing no *X* into the reactor from t = 6 to 12 h, then infused the solution with $[X]_{in}$ = 50 nM into the reactor from t = 12 to 17 h, and finally infused plain buffer into the reactor for the remainder of the experiment (Fig. 2b). As predicted, the fluorescence rose when *X* was pumped in, and decreased when buffer alone was pumped in, equilibrating on the timescale of 2 h.

Lastly, we demonstrated the capacity of the flow reactor to resist transient disturbances to the concentration of *X*. We set up an experiment with $\dot{V}_{in} = 6\,\mu L/min$ and $[X]_{in} = 50\,nM$. After allowing the system to reach steady state, we manually pipetted in 0.2 μL of *X* at a stock concentration of 100 μM, resulting in approximately a 50 nM disturbance to the reaction chamber. We observed that the fluorescence jumped when the disturbance was added, and then returned to the same concentration as before the disturbance (Fig. 2c).

4 Dynamic Boolean strand-displacement logic in a flow reactor

Next we used the flow reactor to perform dynamic molecular logic by introducing a Boolean logic AND gate into our continuous flow reactor, using the Boolean gate motif described in Seelig et al. (2006a). The molecules of the gate were designed to fluoresce only when the two input strands are both present (Fig. 3a, b, Seelig et al. 2006a). We can thus characterize the true/false result of the logic at a given time by measuring the high/low value of fluorescence. Together, the governing equation for the flow reaction (Eq. 2) and the additional mass action reaction terms introduced by the Boolean logic gate reactions (Fig. 3a) can be combined into the coupled set of differential equations given in SI4.

First we tested that the Boolean logic gate gave the correct output response to all four possible combinations of its two binary inputs (Fig. 3c). One problem that can occur if the volumetric flow rates are set too high, relative to the reaction rate constants, is that reactant can enter and leave the reaction chamber quickly enough that there is insufficient time for it to react while in the chamber. To avoid this issue, we imposed bounds on the maximum pumping rate (Eq. 9).

$$\dot{V}_{in} \leq \alpha \cdot V \cdot k_{logic}[ON], \quad (9)$$

where $\dot{V}_{in}$ = volumetric flow rate in, k_{logic} = reaction rate constant for the rate limiting step in the logic reactions, $\alpha = f_{in}/k_{logic} \ll 1$, (we found empirically that values of α = 0.01 worked well), V = volume of the reaction

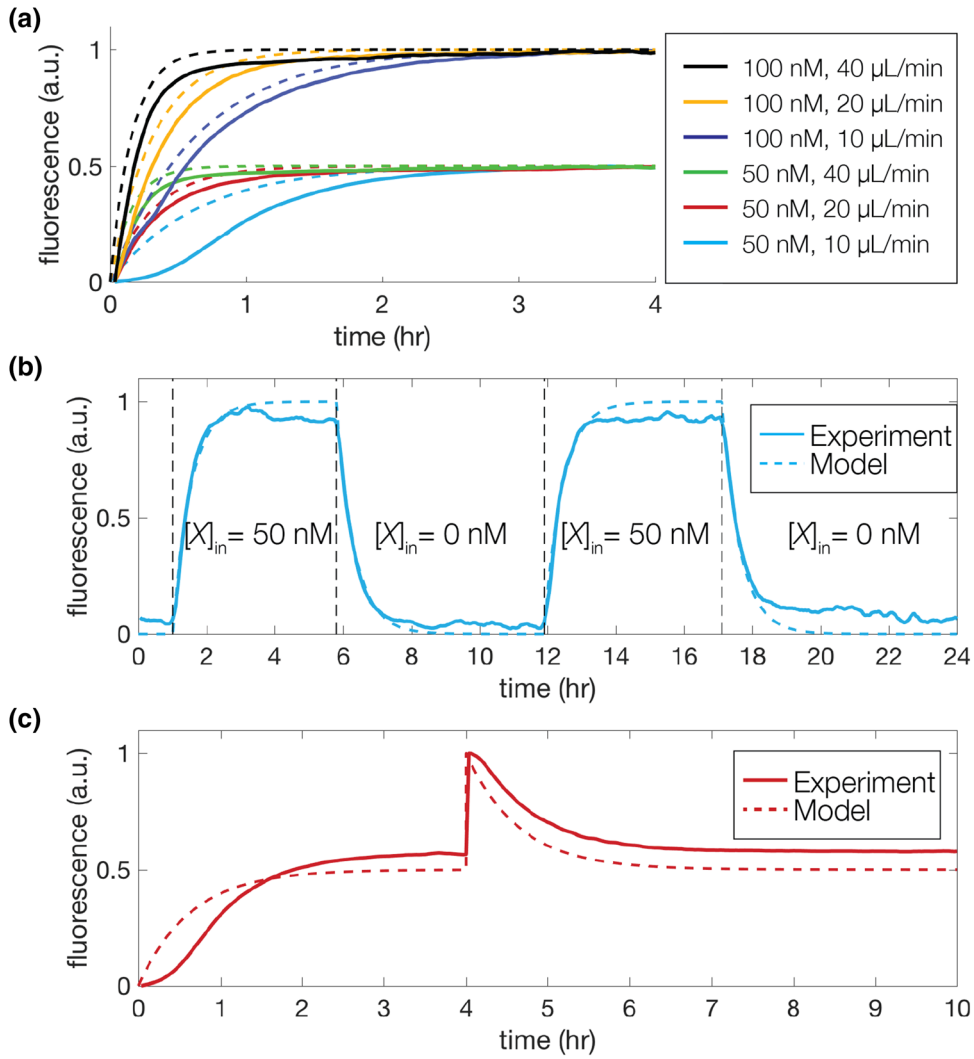

Fig. 2 Control of the concentration of a fluorescently modified DNA strand *X* (47 bases long, labeled with Cy3, see SI 2.3 for sequence) in a reactor via pumps. **a** Steady state normalized fluorescence for different values of $[X]_{in}$ being infused into the reactor and $\dot{V}_{in}$ as shown in legend. Dashed lines indicate model predictions, while solid lines indicate experimental data. **b** Normalized fluorescence as the infused solution is changed over time. After reaching steady state, the concentration of *X* decays to zero after the infusion pump is switched to plain buffer with no fluorescent DNA, then increases when fluorescent DNA is again pumped into the system. Two on/off cycles are shown, with $\dot{V}_{in} = 12\,\mu L/min$ and $[X]_{in} = 50\,nM$ during the on cycles. **c** Experiment showing how the normalized fluorescence in the reactor changes during disturbances. [*X*] first approaches a steady state while $\dot{V}_{in} = 10\,\mu L/min$ for a solution in which $[X]_{in} = 50\,nM$. At t = 4 h, the system is disturbed by pipetting in enough of a concentrated solution of *X* to increase its concentration by 50 nM inside the reaction chamber. After this addition, the steady state fluorescence is eventually restored. Dashed lines show kinetics predicted by Eq. 2 (see SI4). Data is normalized to the maximum fluorescence intensity in each experiment. (Color figure online)

chamber, [ON] = maximum output concentration for the logic gate.

We separated the inputs and the logic gate molecules into two separate infusion lines with equal volumetric flow rates (5 μl/min in each line), to prevent them from reacting until they reached the reaction chamber. To compensate for the resulting dilution of these reactants once they were mixed in the reactor, the concentration of each reactant in its respective infusion line was $N{\cdot}[X]_{in}$, where $N = 2$ was the total number of infusion lines, and $[X]_{in}$ was the desired effective infusion concentration.

In these experiments, one infusion line contained 400 nM AND gate and was turned on for the duration of the experiment. The other line contained the two input molecules at concentrations that denoted either ON, when the infusion line contained 300 nM of an input, or OFF if the infusion line contained none of that input.

To test the dynamic operation of the logic gate (Fig. 3c), we first initialized the system with both inputs in the OFF state, allowing it to run for 2 h to ensure it was at steady state. At t = 2 h, we turned Input 1 ON by increasing its concentration in the input infusion line, while keeping

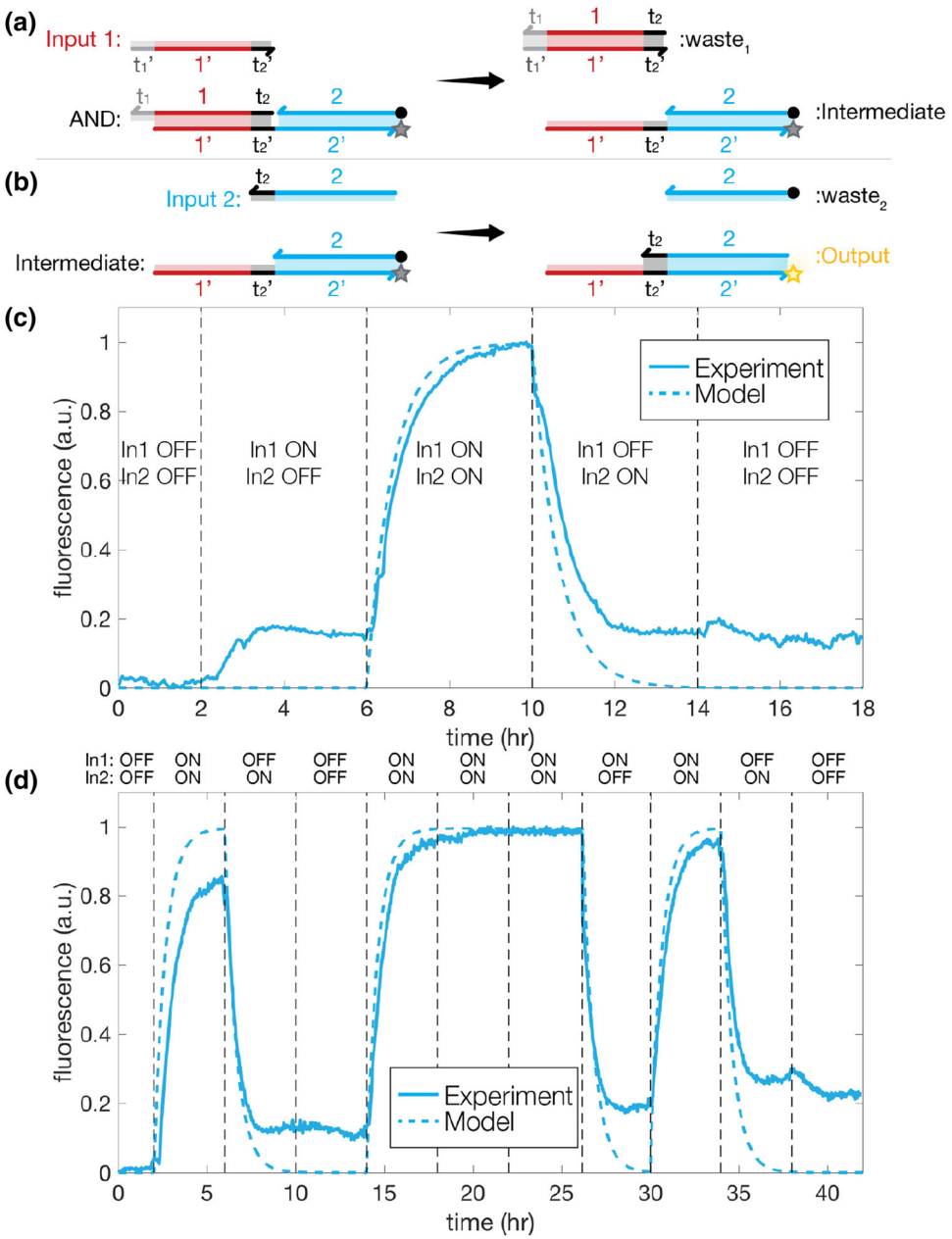

Fig. 3 Operation of a DNA logic gate in a flow reactor. **a**, **b** DNA strand-displacement diagram for the Boolean AND gate (Seelig et al. 2006a, b). DNA strands are represented by lines, and contain short toehold domains (gray, black), and long branch-migration domains (red, cyan). Complementary domains are shown in the same color. The 3' end of each strand is indicated by an arrowhead. Logical evaluation occurs in two reaction steps when both inputs are present. In the first step, (**a**), Input 1 binds to the gray toehold on the AND gate, displacing the red domain and exposing a second toehold (black) in the gate. In the second step, (**b**), Input 2 binds to this newly exposed toehold, displacing the output payload. The output is only released (and thus the fluorescence only changes) when both inputs are present. **c** Experiments showing the AND gate responding to inflow solutions containing all possible ON/OFF combinations of its two inputs (listed in figure) with a volumetric flow rate of $\dot{V}_{in} = 10\,\mu L/min$. In the ON state, inputs were infused at a concentration of $[X]_{in} = 150\,nM$, while in the OFF state $[X]_{in} = 0\,nM$. The dashed line shows the kinetics predicted by Eq. 2 (see SI4). **d** Experiments showing the gate operating for ten different inputs provided in series (separated by dashed vertical lines). The combination of inputs provided during each interval are specified at the top of the plot. The dashed line shows the kinetics predicted by Eq. 2 (see SI4). (Color figure online)

Input 2 OFF. We observed a small increase in fluorescence, but the steady state fluorescence was relatively low, indicating an OFF output. At t = 6 h, we again changed the infusion line to contain both inputs in the ON state. The fluorescence jumped to a high intensity, indicating a correct ON output for the Boolean AND gate. At t = 10 h, we

turned Input 1 OFF, while keeping Input 2 ON, and observed a drop in fluorescence, indicating that the gate had switched back to its correct output state OFF for these inputs. Finally, at t = 14 h, we set both Inputs to OFF, and observed that the fluorescence remained in a low OFF output state. Thus the gate responded correctly to all possible combinations of inputs when they were provided dynamically in the flow reactor.

Finally, we tested the same gate with a more complex set of randomized inputs (Fig. 3d). We supplied Input 1 and Input 2 in the following combinations (t = 0–2 h: I1 = OFF, I2 = OFF), (t = 2–6 h: I1 = ON, I2 = ON), (t = 6–10 h: I1 = OFF, I2 = ON), (t = 10–14 h: I1 = OFF, I2 = OFF), (t = 14–26 h: I1 = ON, I2 = ON), (t = 26–30 h: I1 = ON, I2 = OFF), (t = 30–34 h: I1 = ON, I2 = ON), (t = 34–38 h: I1 = OFF, I2 = ON), (t = 38–42 h: I1 = OFF, I2 = OFF). The output fluorescence dynamically tracked the changing inputs to report the correct Boolean AND output state as the inputs changed over time. In addition to demonstrating that the flow reactor enables the logic gate to operate for many cycles, this experiment also showed how the ON state can be sustained for multiple cycles (t = 14 to 26 h).

5 Conclusion

In this study, we demonstrated that DNA strand displacement reactions can respond dynamically to changing input conditions within a continuous flow reactor. We also developed a protocol for building a relatively simple, easy to manufacture, and affordable flow reactor. Future studies could explore the use of microfluidics to create reactors with smaller volumes, which would reduce the total cost of reagents and could improve robustness.

Microfluidic flow reactors have previously been used to operate other DNA nanotechnology devices, such as DNA origami walkers (Tomov et al. 2017), but to the best of our knowledge, well-mixed continuous-flow stirred-tank reactors have not previously been used to run DNA strand displacement logic circuits. Although flow reactors are convenient means to sustain dynamic reactions, they have several fundamental limitations that closed reactors do not have. First, pumped reactions are not closed systems, in the sense that they depend on flow from outside of the reaction chamber. This may be important in applications where external apparatuses are inconvenient, including many types of in vitro therapeutics. Second, by definition, reactions in well mixed reactors cannot generate stable spatial patterns, so they cannot participate in a broad class of interesting spatially heterogeneous phenomena. Third, since the withdraw pump continuously extracts liquid from the well mixed reactor, anything that we wish to keep inside of the reactor without infusion must be anchored inside of the reactor, or filtered to prevent it from exiting into the withdrawing line. Analogous dynamics to Eq. 2 might be accomplished chemically instead of mechanically, allowing restoration in a closed solution for a finite number of cycles (Scalise and Schulman 2014, 2016), at the cost of increased chemical complexity.

Acknowledgements The authors thank Qi Huang, Yi Li, Samuel Schaffter, and Josh Cole for insightful conversations. This work was supported by NSF-SHF-1527377, DE-SC0010595 for some equipment and reagents, NSF-CCF-1161941 and a grant to the Turing Centenary Project by the John Templeton Foundation to R.S.

Compliance with ethical standards

Conflicts of interest There are no conflicts to declare.

References

Chen X, Briggs N, Mclain JR, Ellington AD (2013a) Stacking nonenzymatic circuits for high signal gain. Proc Natl Acad Sci 110:5386–5391

Chen YJ, Dalchau N, Srinivas N, Phillips A, Cardelli L, Soloveichik D, Seelig G (2013b) Programmable chemical controllers made from DNA. Nat Nanotechnol 8:755–762

Chen YJ, Rao SD, Seelig G (2015) Plasmid-derived DNA strand displacement gates for implementing chemical reaction networks. J Vis Exp 105:e53087

Fern J, Scalise D, Cangialosi A, Howie D, Potters L, Schulman R (2016) DNA strand-displacement timer circuits. ACS Synth Biol 6:190–193

Fratto BE, Katz E (2015) Reversible logic gates based on enzyme-biocatalyzed reactions and realized in flow cells: a modular approach. ChemPhysChem 16(7):1405–1415

Fratto BE, Katz E (2016) Controlled logic gates—switch gate and Fredkin gate based on enzyme-biocatalyzed reactions realized in flow cells. ChemPhysChem 17(7):1046–1053

Genot AJ, Bath J, Turberfield AJ (2011) Reversible logic circuits made of DNA. J Am Chem Soc 133:20080–20083

He JL, Wu ZS, Zhou H, Wang HQ, Jiang JH, Shen GL, Yu RQ (2010) Fluorescence aptameric sensor for strand displacement amplification detection of cocaine. Anal Chem 82(4):1358–1364

Karzbrun E, Tayar AM, Noireaux V, Bar-Ziv RH (2014) Programmable on-chip DNA compartments as artificial cells. Science 345(6198):829–832

Katz E, Fratto BE (2017) Enzyme-based reversible logic gates operated in flow cells. Advances in unconventional computing. Springer, Cham, pp 29–59

Moseley F, Halámek J, Kramer F, Poghossian A, Schöning MJ, Katz E (2014) An enzyme-based reversible CNOT logic gate realized in a flow system. Analyst 139(8):1839–1842

Niederholtmeyer H, Stepanova V, Maerkl SJ (2013) Implementation of cell-free biological networks at steady state. Proc Natl Acad Sci 110(40):15985–15990

Qian L, Winfree E (2011) Scaling up digital circuit computation with DNA strand displacement cascades. Science 332:1196–1201

Qian L, Winfree E, Bruck J (2011) Neural network computation with DNA strand displacement cascades. Nature 475:368–372

Rogers WB, Manoharan VN (2015) Programming colloidal phase transitions with DNA strand displacement. Science 347(6222):639–642

Scalise D, Schulman R (2014) Designing modular reaction-diffusion programs for complex pattern formation. Technology 02:55–66

Scalise D, Schulman R (2016) Emulating cellular automata in chemical reaction–diffusion networks. Nat Comput 15(2):197–214

Seelig G, Soloveichik D, Zhang DY, Winfree E (2006a) Enzyme-free nucleic acid logic circuits. Science 314:1585–1588

Seelig G, Yurke B, Winfree E (2006b) Catalyzed relaxation of a metastable DNA fuel. J Am Chem Soc 128:12211–12220

Semenov SN, Wong ASY, Van Der Made RM, Postma SG, Groen J, Van Roekel HW, de Greef TF, Huck WT (2015) Rational design of functional and tunable oscillating enzymatic networks. Nat Chem 7(2):160

Soloveichik D, Seelig G, Winfree E (2010) DNA as a universal substrate for chemical kinetics. Proc Natl Acad Sci 107:5393–5398

Srinivas N, Parkin J, Seelig G, Winfree E, Soloveichik D (2017) Enzyme-free nucleic acid dynamical systems. Science 358(6369):eaal2052

Takahashi K, Yaegashi S, Kameda A, Hagiya M (2005) Chain reaction systems based on loop dissociation of DNA. DNA Computing Lecture Notes in Computer Science, pp 347–358

Tomov TE, Tsukanov R, Glick Y, Berger Y, Liber M, Avrahami D, Gerber D, Nir E (2017) DNA bipedal motor achieves a large number of steps due to operation using microfluidics-based interface. ACS Nano 11(4):4002–4008

van Roekel HW, Rosier BJ, Meijer LH, Hilbers PA, Markvoort AJ, Huck WT, de Greef TF (2015) Programmable chemical reaction networks: emulating regulatory functions in living cells using a bottom-up approach. Chem Soc Rev 44(21):7465–7483

Zhang DY, Seelig G (2011) DNA-Based Fixed Gain Amplifiers and Linear Classifier Circuits. Lecture Notes in Computer Science DNA Computing and Molecular Programming, pp 176–186

Zhang DY, Turberfield AJ, Yurke B, Winfree E (2007) Engineering entropy-driven reactions and networks catalyzed by DNA. Science 318:1121–1125

Zhang C, Yang J, Xu J (2010) Circular DNA logic gates with strand displacement. Langmuir 26:1416–1419

Zhang DY, Hariadi RF, Choi HM, Winfree E (2013) Integrating DNA strand-displacement circuitry with DNA tile self-assembly. Nat Commun 4:1965